Numerical Findings on the Boundary Layer Transition of Critical-Flow Venturi Nozzles

B. Ünsal[1], K. R. Rathore[2] and E. Koç[1]

[1]TÜBİTAK UME (National Metrology Institute of Turkey)
TÜBİTAK Gebze Yerleşkesi, Barış Mah. Dr. Zeki Acar Cad. No:1, 41470 Gebze / Kocaeli Turkey
[2]Internship student from Gaziantep University, Turkey
E-mail: bulent.unsal@tubitak.gov.tr

Abstract

Presently available information on the boundary layer transition of CFVN (critical flow venturi nozzles) depends only on experimentally measured discharge coefficient variation with Reynolds (Re) number. The investigations reported here aims to add, fluid flow details information of CFVNs transition phenomena, to the existing knowledge for better understanding of the problem. Previous investigations of the authors have shown that various features, of CFVNs, such as discharge coefficient variation with Re number, conjugate heat transfer and flow instability, can be studied numerically by commercial CFD (computational fluid dynamics) packages and numerically obtained results were in good agreement with those of available corresponding experimental cases. For the present investigations, the new turbulence models which have the capability to predict the boundary layer transition were used to simulate the transition occurring within CFVNs. Series of simulation cases were performed for various Re numbers, back pressure ratios (BPR) and nozzle diameters. Presently obtained results indicated that transitional boundary layer can be captured numerically and the comparison of the discharge coefficient results with those of available data is in good agreement.

1. Introduction

Sonic nozzles are widely used to disseminate gas flow rate unit from primary flow metering systems as secondary level calibration standard in gas flow metrology because of their simple construction, easy handling and high accuracy with very good long term repeatability. In the standard ISO 9300 [1], the design and usage of Critical-Flow Venturi Nozzles (CFVN) are well described for Reynolds numbers (Re) 10^5 to 10^7. However, premature unchoking phenomena [2-4], effect of thermal inertia on discharge coefficient [5-7], Re dependency of discharge coefficients [8] and boundary layer transition [9] are the topics where some further research on sonic nozzles are required.

ISO 9300 defines two different discharge coefficient variation functions according to available experimental data. One of them is for normally machined and the other is for accurately machined nozzles. The main difference between them is whether the surface is polished to achieve the required surface roughness or not. Ishibashi [9] named these curves as; aCurve (accurately machined) and nCurve (normally machined). Experimentally measured discharge coefficients variations with Reynolds number (Re) shows that aCurve is valid for laminar boundary layer and nCurve is valid for turbulent boundary results. These experimental results were mostly obtained by accurately machined nozzles and the transition of the discharge coefficient from laminar to turbulent state was clearly shown.

Ishibashi [9] has conducted extensive measurements with several accurately machined nozzles which were produced according to ISO 9300. The results showed three separate transition curves from aCurve to nCurve. The transitional Re range was 0.8×10^6 to 2×10^6. The differences between these were two measurement facilities (constant volume and closed loop facilities) used for the measurements. Based on these results, Ishibashi [9] proposed a sigmoid function, called as sCurve, which shows three separate ranges; laminar range identical to aCurve, turbulent range identical to nCurve and transitional range.

In addition to available extensive experimental discharge coefficient measurements in literature, there are no experimental or numerical data exist on the transitional flow characteristics of CFVNs. Hence, the present investigations, reported here, aims to add some fluid flow details information of CFVNs transition phenomena, to the existing knowledge for better understanding of the problem. To do this, extensive numerical investigations were carried out to characterize boundary layer transition features of Critical Flow Venturi Nozzles (CFVN). For the investigations, nozzle diameters were varied from 0.1 to 30 mm and two dimensional, axisymmetric, steady and unsteady calculations were performed over a broad range of back pressure ratios (BPR) which covers Reynolds number (Re) range of 10^3 to 10^7. The results were summarized in terms of nozzle diameter, boundary layer thickness, and Re.

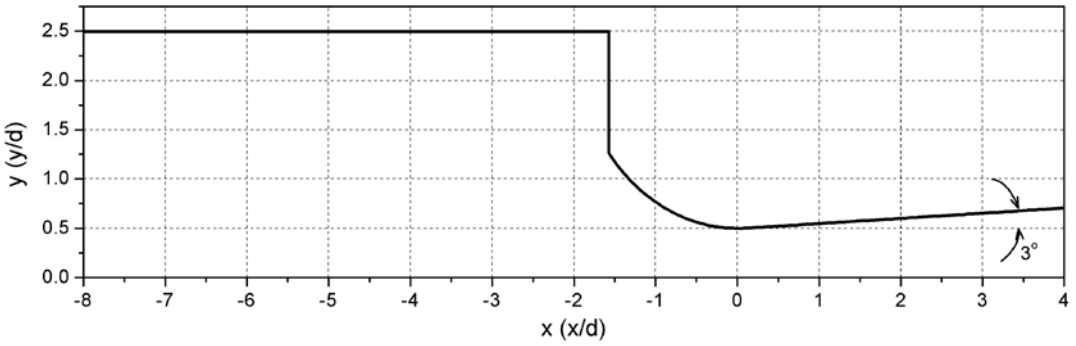

Figure 1: Nozzle geometry.

2. Numerical Calculations

Two dimensional (2D) axisymmetric simulations were performed with the CFD software package ANSYS FLUENT. For the calculation domain, several possibilities were considered for correct prediction of the flow fields by correctly taking into account in-flow effects and also out-flow effects since some back flow and transonic/supersonic exit were expected at some BPR values. As a result of the preliminary predictions, the domain shown in Figure 1 was used for the present investigations.

The mesh size, employed for most of the simulations was around 170,000 with suitable boundary layer resolution according to simulated Re. For heat transfer, adiabatic model is applied with constant wall temperatures, which are equal to incoming flow temperature at the inlet boundary.

Ishibashi [9] has shown experimentally, with accurately machined nozzles, that boundary layer transition along the converging section of the nozzle occurs at around $Re=10^6$. However it was shown by several researchers [10-13] that even at very low Re shock induced boundary layer separation occur along the diverging section of the nozzle which leads turbulent flow. Hence either a direct numerical simulation (DNS) or a turbulence model needed to resolve realistic flow field. For the present investigations, only application of RANS (Reynolds averaged Navier Stokes) turbulence models are considered since objectives of this research cannot be obtained in reasonable time with DNS due to enormous computation time requirements. RANS models offer reasonable computation time with possibility to resolve shock and separation structures. Among these models, k-ε with enhanced wall treatments and SST (shear stress transport) models have options to treat low-Re wall effects to obtain laminar boundary layer along the converging section of the nozzle. SST models have also ability to model intermittency to predict transition with automatic wall functions. Hence, these two models were applied for the present study. Initial calculation results have showed that it was possible with these models to obtain laminar boundary layer and also supersonic separation as experimentally observed by Papamoschou [13].

Steady state simulations were conducted for nozzle diameters of 0.1, 3, 5, 10, 15, 20 and 30 mm. At some selected Re, transient simulations were also done to compare the time averaged flow fields and discharge coefficients with corresponding steady state results. These comparisons were in good agreement so that all the results presented here can be obtained through steady state solutions.

3. Results

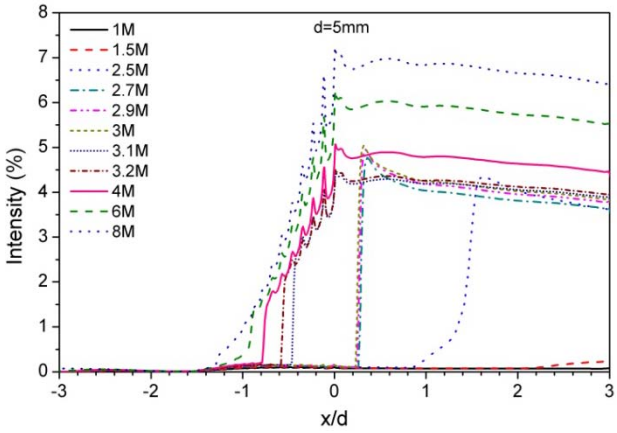

Figure 2: Turbulence intensity variation along the wall for 3 mm diameter nozzles.

In Figure 2, turbulence intensity variation along the nozzle wall is shown for 5 mm diameter nozzle. In the figure, x axis is normalized with nozzle diameter and the position zero stands for the throat location (see Figure 1). The computations for 5 mm nozzle was performed at 22 Re points and cover Re range of $2x10^5$ to $1x10^7$. However, in the figure only 11 Re results were plotted for better view. As the figure indicates, the boundary layer transition initially takes places along the diffuser and while the Re increases, the transition location moves against flow direction until the nozzle inlet. Boundary layer at the throat becomes turbulent after around $Re=3.5x10^6$.

For some selected Re, throat velocity profiles for 5 mm nozzle are shown in Figure 3. The profiles differ only near to the wall. For better visualization of the profiles near to wall, U^+ vs y^+ plot is shown in Figure 4. This figure also indicates viscous, buffer and log layers of a

turbulent flow. Within the viscous layer (also called as laminar layer) all the profiles collapse. The difference between laminar and turbulence can be identified in buffer and log layers. Within the log layer, the turbulent profiles show logarithmic variation as indicated in the figure.

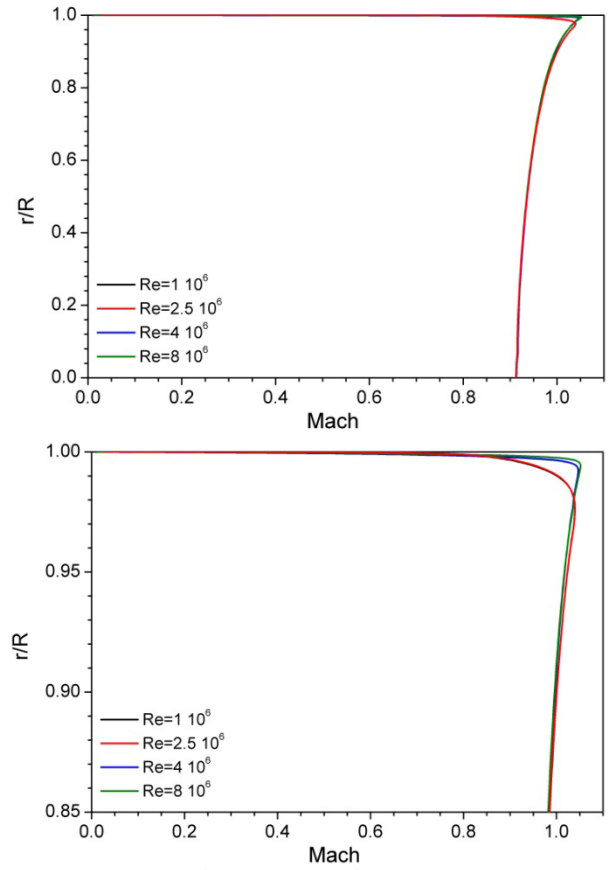

Figure 3: Velocity profiles at the throat for 5 mm nozzle. Bottom figure is showing the profiles near to wall.

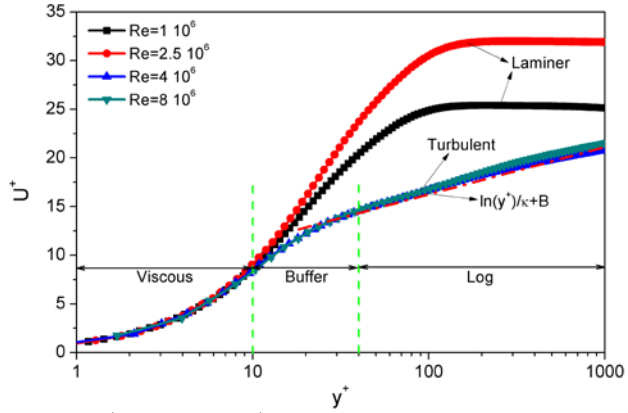

Figure 4: U^+ variation with y^+ at the throat for 5 mm nozzle.

In Figure 5, variation of discharge coefficient with Re is shown for 5 mm nozzle. In this figure the solid line is the sCurve which represents laminar and turbulent variation according to ISO 9300 and also transitional range as reported by Ishibashi [9]. As the figure indicates, the transitional Re for 5 mm nozzle is around 3.5×10^6. The results show very good agreement with sCurve within laminar and turbulent regimes. However the transition point for 5 mm nozzle differs from the transitional range suggested by Ishibashi [9].

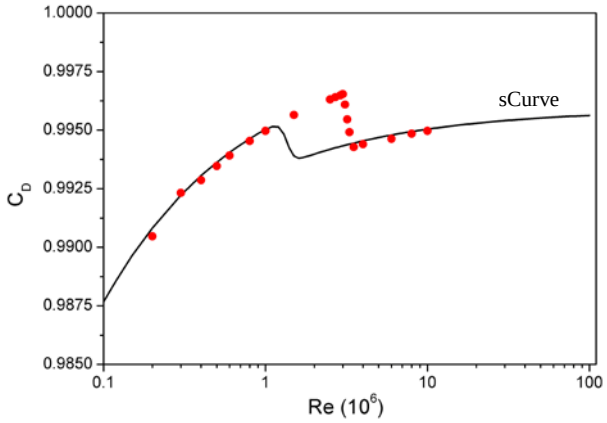

Figure 5: Variation of discharge coefficient with Re for 5 mm nozzle.

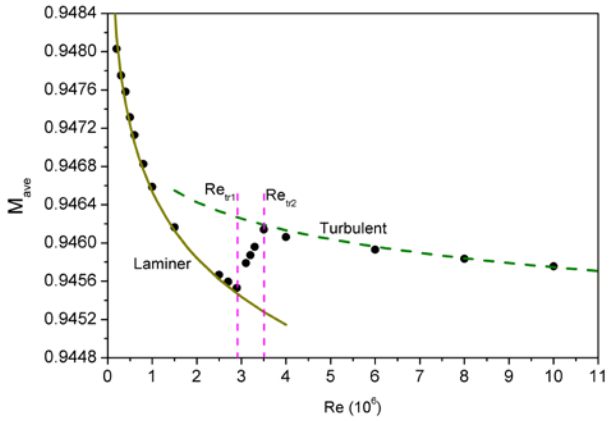

Figure 6: Area averaged Mach number variation with Re for 5 mm nozzle.

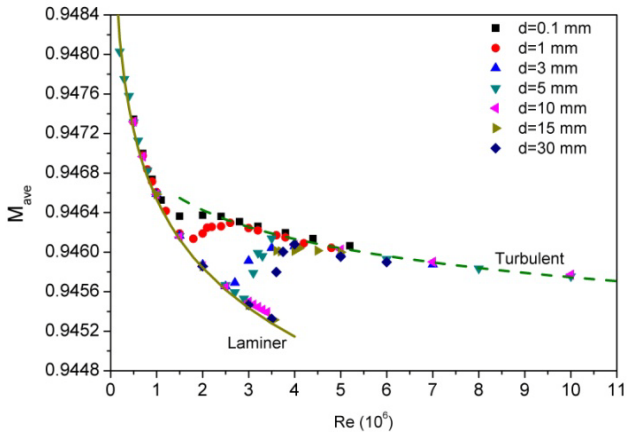

Figure 7: Area averaged Mach number variation with Re.

For determination of the transitional Re range, area averaged Mach number can also be used at any cross section. Figure 6 is showing area averaged Mach number variation with Re for 5 mm nozzle. In this figure two transitional Re can be identified as Re_{tr1} which is the start of the transitional regime from laminar state and Re_{tr2} as the end of the transitional regime. Figure 7 is showing the same as figure 6 but for all the diameters investigated. Laminar and turbulent regimes are indicated with lines as shown in both figures. These lines were obtained through curve fittings to laminar and turbulent results.

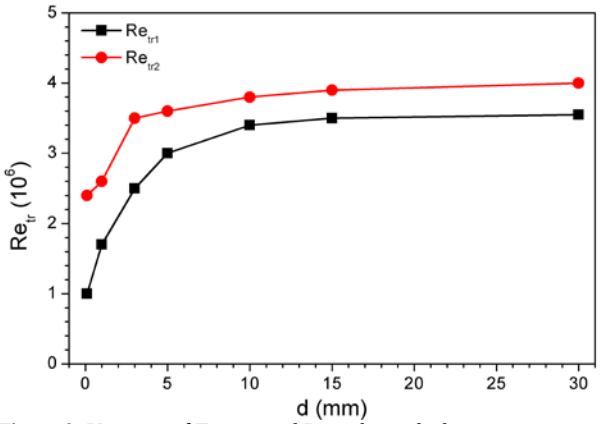

Figure 8: Variation of Transitional Re with nozzle diameter.

Transitional Re (Re_{tr1} and Re_{tr2}) extracted from Figure 7 is plotted in Figure 8. This figure indicates that for large diameters (e.g. 10 mm and above) transitional Re do not change much. For the diameters lower than 10 mm, while the diameter decreases the rate of transitional Re decrease increases.

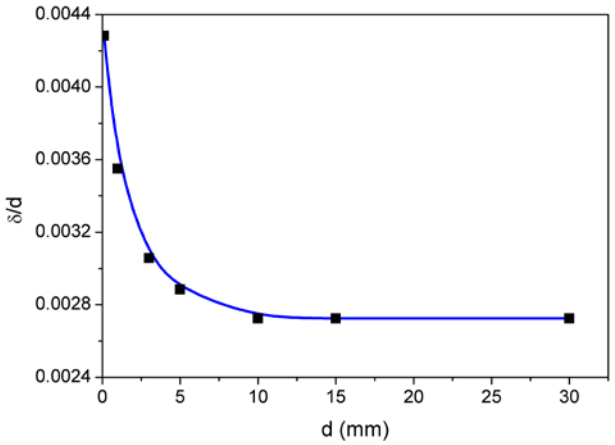

Figure 9: Normalized throat boundary layer thickness variation with pipe diameter.

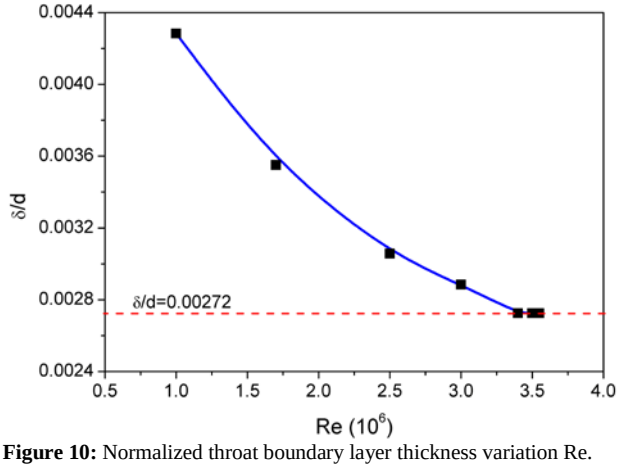

Figure 10: Normalized throat boundary layer thickness variation Re.

In Figure 8 the transitional Re results were plotted against throat diameter but actually the diameter should be normalized with another length variable. Boundary layer thickness can be used to normalize the throat diameter. In Figure 9, normalized boundary layer thickness at the throat with throat diameter is shown. In this figure the data represents the values obtained at the Re_{tr1}. As the figure clearly indicates, for diameters 10 mm and above the normalized boundary layer thickness is almost constant. For lower throat diameters the values are increasing while the throat diameter decreases.

Variation of normalized boundary layer thickness at the throat with Re is shown in Figure 10. From the figures 9 and 10, it can be concluded that for diameters above 10 mm the transitional Re is almost constant at around $3.5x10^6$ and this corresponds to a critical boundary layer thickness as indicated in Figure 10.

4. Conclusions

Axisymmetric, steady and 2D CFD calculations were performed for nozzle diameters 0.1 to 30 mm to investigate boundary layer transition of CFVNs. From the results presented here, the following conclusions can be made;

- Boundary layer transition takes place initially within the diffuser section (see Figure 2). With increasing Re, the transition location moves against flow direction until the nozzle inlet section.
- Laminar and turbulent velocity profiles at the throat, show only difference near to wall (see figures 3 and 4).
- Numerically calculated discharge coefficients are in good agreement with ISO 9300 and the sCurve suggested by Ishibashi [9].
- The transitional Re (Re_{tr1} and Re_{tr2} as defined in Figure 6) show diameter dependence for diameters below 10 mm. But for 10mm and above transitional Re stays almost constant (see figures 8, 9 and 10). The measurement results of Ishibashi [9] indicate no diameter dependence. However his results covers only large diameters and he did not provide diameter information.
- For CFVN diameters 10 mm and above, there is a critical normalized boundary layer thickness as indicated in Figure 10. This critical thickness corresponds to a transitional Re of around $3.5x10^6$. For diameters below 10 mm there is almost a linear relation between Re and normalized boundary layer thickness as can be seen from Figure 10.

References

[1] ISO 9300, "Measurement of gas flow by means of critical flow Venturi nozzles", 2nd edition, 2005

[2] R W. Caron, C. L. Britton, T. M. Kegel, "The premature unchoking phenomena of critical flow venturis", MSC, 2004

[3] S. I. Nakao, M. Takamoto, “Choking phenomena of sonic nozzles at low Reynolds numbers”, Flow Meas. Instr., 2000
[4] H. Hu, C. Wang, L. Cui, C. Li, T. Meng, "Experimental study on critical back pressure ratio of sonic nozzle at low Reynolds number”, 8th ISFFM, 2012
[5] N. Bignell and Y.M. Choi, "Thermal effects in small sonic nozzles", Flow Meas. Instr., Vol. 13, pp. 17-22, 2002
[6] B. Unsal, K. Park, H. Kaykisizli, “Investigations on the effect of thermal inertia on sonic nozzle discharge coefficient”, 16th International Flow Measurement Conference 2013, FLOMEKO 2013, pp. 512-515. 2013
[7] B. Unsal, U. Caliskan, “Numerical assessment of discharge coefficient, and wall temperature dependence of discharge coefficient for critical-flow venturi nozzles”, 9th ISFFM, 2015
[8] M, Ishibashi, M, Takamoto “Discharge coefficient of super-accurate critical nozzles accompanied with the boundary-layer transition measured by reference super-accurate critical nozzles connected in series”, ASME FED Summer Meeting (FEDSM2001), paperNo.18036, 2001
[9] M, Ishibashi “Discharge coefficient equation for critical-flow toroidal-throat venturi nozzles covering the boundary layer transition regime”, Flow Meas. & Instr., Vol. 44, pp. 107-121, 2015
[10] K. B. M. Q. Zaman, T. J. Bencic, M. M. Clem, A. F. Fagan, “Schock induced boundary layer separation in C-D nozzles and its impact on jet noise”, 49th AIAA Aerospace Sciences Meeting, Orlando, 2011
[11] B. J. Olson, S. K. Lele, “A mechanism for unsteady separation in over-expanded nozzle flow”, Phy. of Fluids, 25, 110809, 2013
[12] B. Unsal, U. Caliskan, “Flow stability of critical flow venturi nozzles”, 9th ISFFM, 2015
[13] D. Papamoschou, “Mixing enhancement using axial flow”, AIAA Paper 2000-0093, 2000